DALTON
FULL PAPER

Patterned crystallisation on self-assembled monolayers with integrated regions of disorder †

Joanna Aizenberg

Bell Laboratories/Lucent Technologies, 600 Mountain Ave., Murray Hill, NJ 07974, USA. E-mail: jaizenberg@lucent.com

Received 27th April 2000, Accepted 2nd June 2000
First published as an Advance Article on the web 10th October 2000

This paper describes the engineering of patterned calcite films using templating by self-assembled monolayers (SAMs) supported on micropatterned mixed metal substrates. The substrates were prepared by deposition of one metal (Au, Ag) onto the surface of another metal (Au, Ag) through a stencil or photoresist masks. The micropatterning arises from the generation of disordered regions in SAMs at the interfaces between the two metals, where structurally different SAMs meet. The mechanism of diffusion-limited nucleation on these substrates that governs the formation of different patterns of calcite crystals, crystalline outlines of the underlying patterns, densely crystallised islands and patterned oriented films, is discussed. The ability to control patterned crystallisation with sub-50 nm resolution can find applications in the fabrication of crystalline inorganic materials with complex form.

Introduction

Crystalline inorganic materials with microscale regularity have important applications in microelectronics, optics, information storage, biomedical implants, catalysis and separation technologies.[1] The development of new methods of the pattern control on a sub-micron scale is, therefore, a challenging problem in crystal engineering. It has been shown that patterned inorganic materials can be templated by supramolecular assemblies of biological or synthetic organic macromolecules.[2] A number of interesting studies have discussed the preparation of nano- and micro-patterned inorganic structures using supramolecular lipid or protein cages,[3] bacterial fibres,[4] reverse microemulsions, liquid-crystal and surfactant aggregates,[5] and diblock copolymers.[6] Since the architecture of the surfacing crystalline phase is defined by the structure of the underlying supramolecular assembly, the goal of many studies has been the development of convenient techniques for the fabrication of arbitrarily patterned organic substrates.

Microcontact printing (μCP) of self-assembled monolayers (SAMs) of alkanethiols on gold, silver and copper or of silanes on silica is a simple, broadly applicable technique for derivatising surfaces on a sub-micron scale.[7] Microprinted SAMs served as organic substrates for directing various area-selective interfacial processes, such as localised cell and protein adhesion,[8] wetting,[9] patterned deposition of polymers[10] and inorganic materials.[11] It has been demonstrated that by varying the functionality of the SAM, the size and geometry of the features on the patterned surface, and the concentration of the crystallising solution, one can fabricate arbitrarily patterned arrays of calcite crystals with controlled crystallographic orientation, density and pattern of nucleation, and crystal sizes.[12,13] The feature sizes formed by μCP are, however, limited to >100–200 nm, because of the diffusion of ink molecules in the printing stage and the fragility of the ordered regions in SAMs.[14]

Recently a new method for patterning SAMs using mixed metal substrates was suggested.[15] Highly localised regions of disorder in SAMs are generated at the edges between different metals in topographically patterned evaporated metal films. These regions provide active sites for the preferential exchange of molecules in SAMs, formation of condensation figures, and selective etching of the underlying metal films with sub-50-nm resolution.[15,16] Here the use of SAMs patterned with regions of disorder as templates for inorganic crystal engineering is described. Selective nucleation at the disordered regions resulted in a patterned calcite growth in the form of outlines of the underlying surface, dense crystalline islands and patterned interconnected films.

Experimental

Silicon wafers or glass slides were coated with 2 nm of Ti, to promote adhesion, and then typically with 50 nm of metal (Ag, Au) using an electron beam evaporator (base pressure 10^{-7} Torr). The second metal (Ag, Au) was then deposited using a stencil, *e.g.* transmission electron microscopy (TEM) grid, or photoresist mask. In the latter case the photoresist pattern of a desired geometry was formed on the surface of the first metal using conventional lithographic techniques and applied as a screen for the evaporation of the overlayer of a second metal. The photoresist was then dissolved in acetone revealing the micropatterned metal surface.

The topographically micropatterned metal substrates were exposed to a 10 mM solution of $HS(CH_2)_{15}CO_2H$ in ethanol for 1 hour, rinsed with ethanol and placed into $CaCl_2$ solution in a closed desiccator containing vials of solid $(NH_4)_2CO_3$. The substrates were positioned upside down on supports to prevent non-specific crystallisation induced by gravity. Calcite crystals were formed by diffusion of carbon dioxide vapor into the $CaCl_2$ solution, according to reactions (1)–(3). The concentration of the $CaCl_2$ solution and the crystallisation time were varied in different experiments. The substrates decorated with

$$(NH_4)_2CO_3 \longrightarrow 2NH_3\,(g) + CO_2\,(g) + H_2O \quad (1)$$

$$CO_2 + Ca^{2+} + H_2O \longrightarrow CaCO_3\,(s) + 2H^+ \quad (2)$$

$$2NH_3 + 2H^+ \longrightarrow 2NH_4^+ \quad (3)$$

† Based on the presentation given at Dalton Discussion No. 3, 9–11th September 2000, University of Bologna, Italy.

DOI: 10.1039/b003400m

calcite crystals were rinsed with double-distilled water and examined in a scanning electron microscope (JEOL 6400).

Results and discussion

The experimental set-up is shown in Fig. 1. Two methods were used to fabricate micropatterned mixed metal substrates: (a) deposition of a metal (M_2) onto the surface of another metal (M_1) through a micropatterned stencil mask, *e.g.* a TEM grid (Fig. 1a); (b) deposition of M_2 onto M_1 whose surface had been patterned with photoresist using conventional lithographic techniques, followed by lift-off of the photoresist layer (Fig. 1b). SAMs of $HS(CH_2)_{15}CO_2H$ were formed on these patterned substrates and used as nucleation templates for calcite crystallisation.

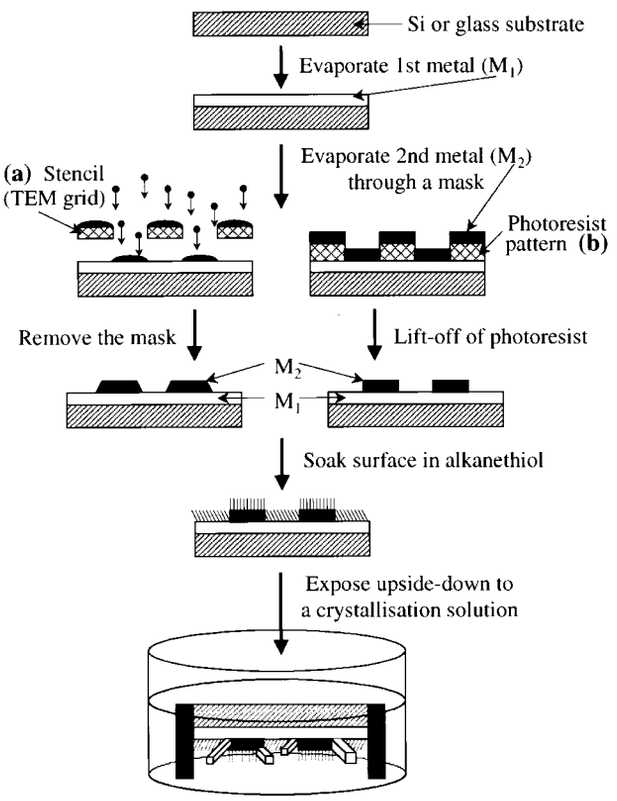

Fig. 1 Schematic representation of the experimental procedure for the crystallisation on SAMs supported on mixed metal substrates prepared by deposition of the overlayer of a metal on the surface of another metal using a stencil (a) and a photoresist mask (b).

Fig. 2 shows scanning electron micrographs (SEMs) of patterns of calcite crystals grown on SAMs. Control crystallisation experiments with micropatterned metal substrates bearing no SAM were carried out for comparison. It is clearly seen that substrates supporting SAMs generated patterns of crystals that replicated the structure of the underlying surface (Fig. 2a,c). The bare micropatterned substrates did not induce preferential nucleation anywhere on the surface (Fig. 2b,d). This result indicates that patterned crystallisation does not arise from the changes in topography of the surface and is only induced by the local differences in the structure of SAMs when they are supported on micropatterned mixed metal substrates.

The mechanism for the formation of structurally different regions in SAMs is shown in Fig. 3. The atomic force microscopy (AFM) study of the topography of the patterned metal films shows that for the stencil patterning the interface between the two metals is not sharp and the local curvature is about 5–10°, presumably due to the shadowing from the edges of the mask (Fig. 3a). The use of the photoresist mask results in the formation of sharp interfaces between the two metals with topological steps of about 70–80° (Fig. 3b). It has been shown that alkanethiol molecules self-assemble on different metals ($M_2 \neq M_1$) into monolayers having different lattice, tilt and twist angles.[17] At the region where two structurally different SAMs meet, the order in the SAM is reduced[15] for both substrate types, fabricated using the stencil (Fig. 3a) and the photoresist masks (Fig. 3b). When $M_2 = M_1$ in the former case no disorder is formed in the SAM since the surface is nearly flat locally (Fig. 3a), whereas in the latter case the formation of sharp topographical steps is sufficient for inducing the local disorder in a supported SAM (Fig. 3b). Diffusion and mixing of two different metals may also contribute to the local disorder in the supported SAM.

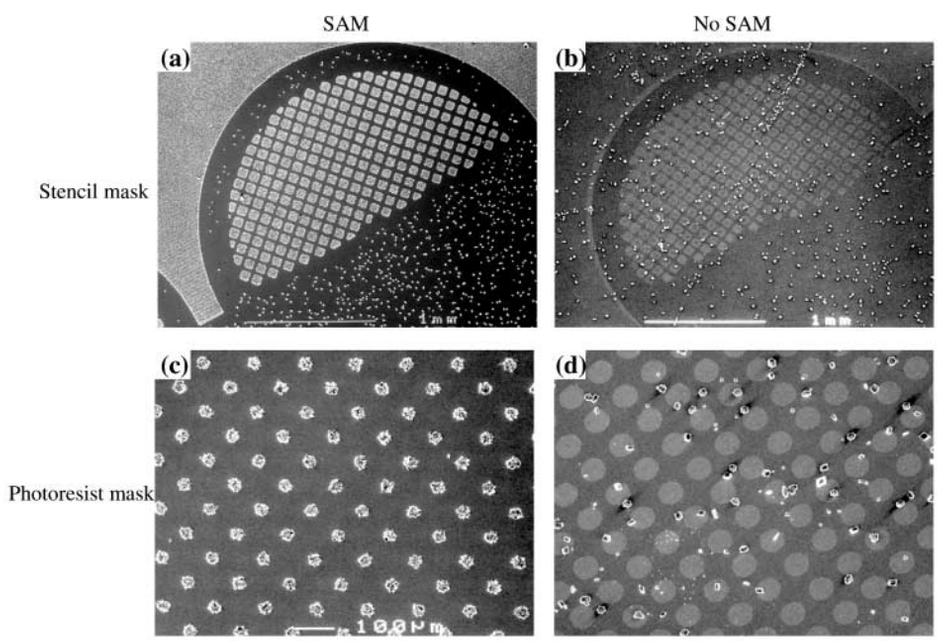

Fig. 2 Sample SEMs of calcite crystals grown on mixed metal substrates. (a) Patterned crystallisation on a SAM of $HS(CH_2)_{15}CO_2H$ supported on a substrate which consisted of silver islands deposited on Au through a TEM grid. (b) Non-patterned crystallisation of randomly oriented calcite crystals induced by the same micropatterned metal substrate as in (a) supporting no SAM. (c) Patterned crystallisation on a SAM of $HS(CH_2)_{15}CO_2H$ supported on a substrate which consisted of silver islands deposited on Au through a photoresist mask. (d) Non-patterned crystallisation of randomly oriented calcite crystals induced by the same micropatterned metal substrate as in (c) supporting no SAM (same magnification).

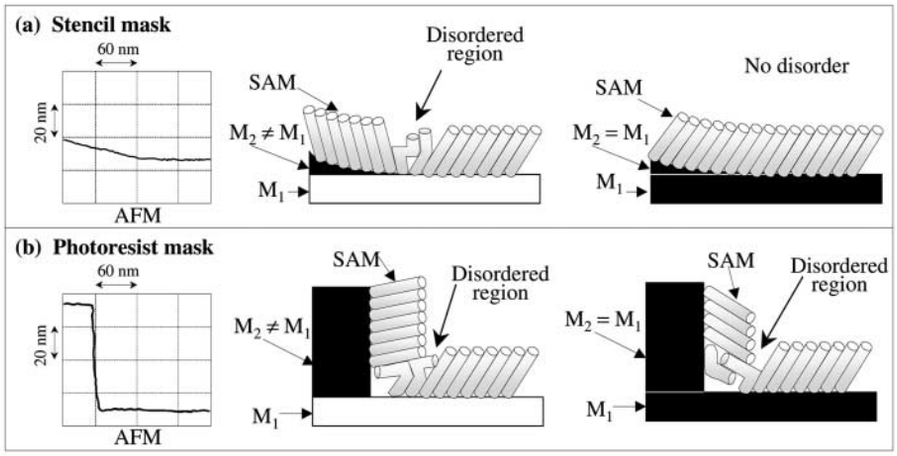

Fig. 3 Structures of the interfacial regions between two metals patterned using a stencil (a) and a photoresist mask (b).

Heterogeneous nucleation is extremely responsive to the structure and order of the inductive surface.[18,19] Control crystallisation experiments with SAMs that were intentionally damaged by an electron beam prior to crystallisation showed that the induction time for nucleation at the disordered, damaged regions is shorter than that for the ordered areas. We have also performed detailed statistical analysis of calcite crystals grown on SAMs with increasing density of defects. The results of this study[19] showed that with decrease of the immersion time of metal substrates in the thiol solution (*i.e.* with increase of the defect density in SAMs) the induction time of nucleation and the percentage of oriented crystals[13] decrease. Therefore, when SAMs with integrated regions of disorder are used as nucleation templates, patterned crystallisation that replicates the ornament of the disordered regions in the underlying SAMs results (Fig. 2a,c).

The mechanism of the pattern formation is illustrated in detail in Fig. 4. The analysis of the decorated surfaces at different stages of the crystallisation experiment showed that the disordered regions in SAMs provide the first nucleation sites, in agreement with the results of the control experiments described above. The flux of ions to the growing crystals induces a gradient of concentration in the vicinity of the interfaces between the two metals and causes the formation of a depletion region L_d where nucleation does not occur (Fig. 4a), eqn. (4), where D

$$L_d \approx (D/F)^{1/4} \quad (4)$$

($cm^2\ s^{-1}$) is a diffusion coefficient and F ($cm^{-2}\ s^{-1}$) is a flux of ions.[12,20] The profiles of concentration of the crystallisation solution, $c(x)$, in the vicinity of the border between two different metals is shown in Fig. 4b. The profiles were derived using the diffusion equation (5) and assuming zero concentration of

$$\partial c/\partial t = D\partial^2 c/\partial x^2 \quad (5)$$

solution at the disordered region, that is assuming that all the ions that reach the surface of the crystals growing there stick irreversibly. The concentration profiles are steeper for the surface that shows higher nucleating activity and shorter induction time t_M (surface M_2 in Fig. 4b). Crystallisation does not occur within the distances L_{d1} and L_{d2} ($L_{d1} > L_{d2}$) from the disordered region where the local effective concentration of the solution (c_{eff}) is below saturation (c_{sat}). The nucleation resumes for $x > L_d$, where $c > c_{sat}$ (Fig. 4a,b).[12] One can create different crystallisation patterns by controlling either the sizes of the metal features on the surface or the concentration of the crystallising solution. *For low concentration* of the solution, when the effective concentration over the entire surface is below saturation (bold lines in Fig. 4c), crystallisation will be restricted only to the *disordered regions* in SAMs. *For inter-*

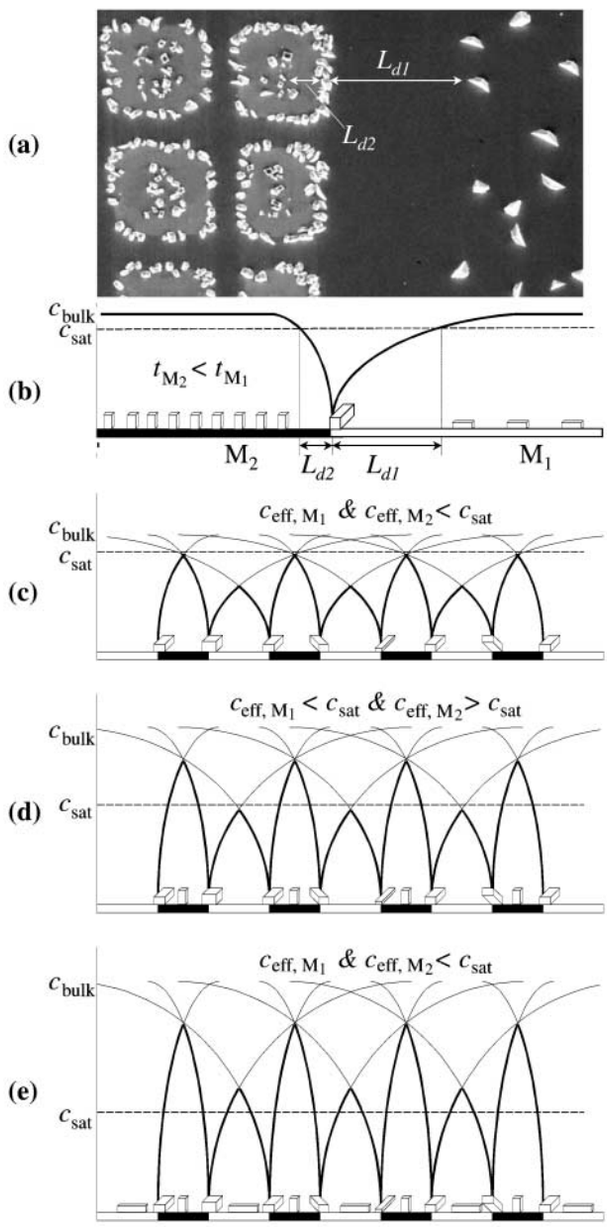

Fig. 4 Illustration of the mechanism of patterned crystallisation induced by SAMs with integrated regions of disorder. (a) SEM image of the fragment of the micropatterned surface decorated with calcite crystals at the edge of the grid pattern. (b) Calculated profiles of concentration of the crystallising solution in the vicinity of the disordered region where the nucleation occurs. (c)–(e) Pattern control by adjusting the concentration of the crystallising solution (see text for details).

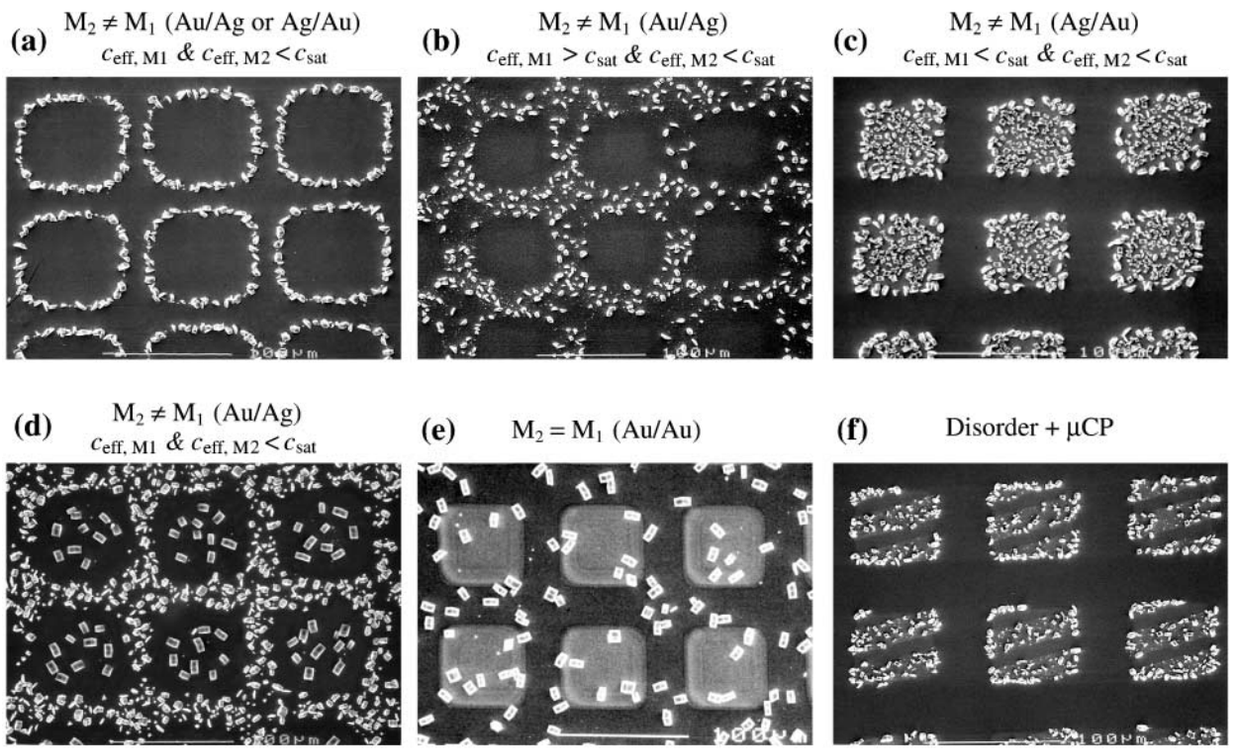

Fig. 5 (a)–(d) Patterned calcite formation on SAMs of $HS(CH_2)_{15}CO_2H$ supported on substrates that were micropatterned with Au and Ag using a stencil mask (TEM grid). The sequence of metal deposition and the concentration range are indicated. Note the differences in the densities of nucleation, sizes and crystallographic orientation of crystals grown on different metals. (e) Non-patterned nucleation of oriented calcite crystals on SAMs of $HS(CH_2)_{15}CO_2H$ supported on the gold substrate micropatterned with the gold islands. (f) Complex ornament of crystals formed on a mixed metal substrate further patterned using μCP.

mediate concentrations of the solution, when c_{eff} over the more active surface is above saturation and c_{eff} over the less active surface is below saturation (bold lines in Fig. 4d), crystals will decorate the *more active regions*. *For high concentrations* of the solution, when c_{eff} over the entire surface is above saturation (bold lines in Fig. 4e), crystallisation will take place on the *entire surface*.

Fig. 5 shows the application of the described principles to the fabrication of complex micropatterns of calcite crystals on substrates prepared by the stencil method. The substrates were patterned with Au and Ag deposited in different sequences through a TEM grid and derivatised with the SAMs of $HS(CH_2)_{15}CO_2H$. For $c < 10$ mM, selective crystallisation at the boundaries between the two different metals took place (Fig. 5a). The formation of these crystalline outlines of the underlying regions of disorder in SAMs corresponds to the mechanism shown in Fig. 4(c). It has been shown earlier that SAMs of $HS(CH_2)_{15}CO_2H$ supported on Ag and Au induce oriented nucleation of calcite from the (012) and (015) crystallographic planes respectively.[12,13] The rate and density of nucleation of calcite are higher on SAMs of $HS(CH_2)_{15}CO_2H$ supported on Ag than on Au.[13,15] In agreement with these observations, crystallisation using solutions of intermediate concentrations ($c = 20$–40 mM) resulted in the preferential decoration of the silver regions of the surfaces. Calcitic mesh oriented in the [012] crystallographic direction was formed when the islands of Au were deposited on the silver film (Fig. 5b), and oriented calcitic islands were fabricated for the reverse deposition sequence (Fig. 5c). The formation of crystalline patterns shown in Fig. 5(b,c) corresponds to the mechanism depicted in Fig. 4(d). For $c > 50$ mM, crystallisation occurred on the entire surface (Fig. 5d), according to the mechanism in Fig. 4(e). The crystal patterns on the regions of Ag and Au had the expected characteristic nucleation densities, crystal sizes and crystallographic orientations.[12,13,15] When $M_2 = M_1$ no preference for nucleation from the interfacial regions was observed, irrespective of the concentration of the crystallising solution, indicative of the absence of disorder in the SAM as was suggested in Fig. 3(a). The crystallographic orientation of the forming crystals, [015], was uniform and characteristic of that observed on the corresponding non-patterned substrates[13] (Fig. 5e).

For micropatterned substrates fabricated using photoresist masks the interfacial regions of SAMs are disordered for any metal combination (see Fig. 3b). Accordingly, at low concentration of the solution, crystalline outlines of the underlying patterns were generated for both $M_2 = M_1$ and $M_2 \neq M_1$ (Fig. 6a). At higher concentrations, isolated islands of oriented crystals (Fig. 6b) or oriented interconnected crystalline film (Fig. 6c) formed. A significant advantage of lithographically patterned metal films is the ability to form features of sub-micron sizes.

By combining the described technique with μCP one can fabricate micropatterned surfaces of higher hierarchy. Fig. 5(f) presents an example of a complex calcitic pattern grown on a Ag/Au substrate stamped with lines of $HS(CH_2)_{15}CO_2H$ and filled with $HS(CH_2)_{15}CH_3$. Crystals nucleate only on the carboxylic acid terminated regions located within the silver islands of the patterned surface.

Conclusion

The successful use of micropatterned mixed metal substrates supporting SAMs as templates for inorganic crystal engineering has been demonstrated. The disordered regions that form in these SAMs at the interfaces between different metals are tens of nanometers wide and, therefore, they induce highly localised crystal nucleation. Further crystal growth is governed by the diffusion-limited mechanism. Using calcite crystallisation as an example, it was shown that, by adjusting the concentration of the crystallising solution or the sizes of features on the surface, it is possible to fabricate arbitrary, high-resolution patterns of microcrystals with controlled sizes, orientation and densities of nucleation in each part of the surface. The generation of

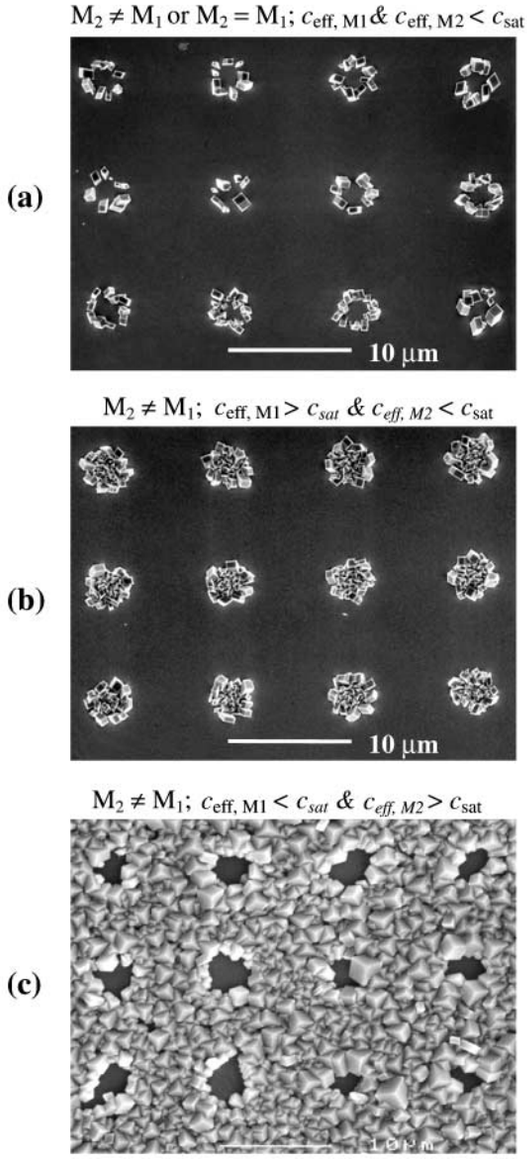

Fig. 6 Fabrication of the crystalline outlines of the patterned substrates (a), crystalline islands (b) and interconnected crystalline film (c) using SAMs of $HS(CH_2)_{15}CO_2H$ supported on substrates that were micropatterned with Au and Ag through a photoresist mask. The photoresist pattern consisted of cylinders with a diameter of 3 μm and periodicity of 10 μm. The sequence of metal deposition and the concentration range are indicated.

crystalline outlines of the underlying patterns is especially interesting since they cannot be formed by other crystallisation techniques. This method, combined with μCP, makes it possible to generate complex crystalline patterns of higher hierarchy. We believe that the described approach will have broad applications in the synthesis of patterned crystalline films of various inorganic materials.

Acknowledgements

I thank Professor G. M. Whitesides and Dr A. J. Black for their valuable contribution to this study.

References

1 W. M. Moreau, *Semiconductor Lithography: Principles and Materials*, Plenum, New York, 1988; F. Cerrina and C. Marrian, *Mater. Res. Soc. Bull.*, 1996, **12**, 56; A. H. Heuer, D. J. Fink, V. J. Laraia, J. L. Arias, P. D. Calvert, K. Kendall, G. L. Messing, J. Blackwell, P. C. Rieke, D. H. Thompson, A. P. Wheeler, A. Veis and A. I. Caplan, *Science*, 1992, **255**, 1098; S. I. Stupp and P. V. Braun, *Science*, 1997, **277**, 1242; B. J. J. Zelinsky, C. J. Brinker, D. E. Clark and D. R. Ulrich, *Better Ceramics Through Chemistry*, Materials Research Society, Pittsburg, 1990; S. Mann and G. A. Ozin, *Nature* (*London*), 1996, **382**, 313; C. R. Kagan, D. B. Mitzi and C. D. Dimitrakopoulos, *Science*, 1999, **286**, 945; H. Yang, A. Kuperman, N. Coombs, S. MamicheAfara and G. A. Ozin, *Nature* (*London*), 1996, **379**, 703; N. A. Peppas and R. Langer, *Science*, 1994, **263**, 1715; D. W. Breck, *Zeolite Molecular Sieves*, Krieger, Malabar, FL, 1984.

2 M. Alper, P. D. Calvert, R. Frankel, P. C. Rieke and D. A. Tirrell, *Materials synthesis based on biological processes*, Materials Research Society, Pittsburg, 1991; S. Mann, *Nature* (*London*), 1993, **365**, 499; S. Mann, D. D. Archibald, J. M. Didymus, T. Douglas, B. R. Heywood, F. C. Meldrum and N. J. Reeves, *Science*, 1993, **261**, 1286; S. Mann, S. L. Burkett, S. A. Davis, C. E. Fowler, N. H. Mendelson, S. D. Sims, D. Walsh and N. T. Whilton, *Chem. Mater.*, 1997, **9**, 2300; B. C. Bunker, P. C. Rieke, B. J. Tarasevich, A. A. Campbell, G. E. Fryxell, G. L. Graff, L. Song, J. Liu, J. W. Virden and G. L. McVay, *Science*, 1994, **264**, 48; E. Evans, H. Bowman, A. Leung, D. Needham and D. Tirrell, *Science*, 1996, **273**, 933; J. H. Fendler and F. C. Meldrum, *Adv. Mater.*, 1995, **7**, 607.

3 F. C. Meldrum, B. R. Heywood and S. Mann, *Science*, 1992, **257**, 522; F. C. Meldrum, V. J. Wade, D. L. Nimmo, B. R. Heywood and S. Mann, *Nature* (*London*), 1991, **349**, 684; D. D. Archibald and S. Mann, *Nature* (*London*), 1993, **364**, 430; S. Lafont, H. Rapaport, G. J. Somjen, A. Renault, P. B. Howes, K. Kjaer, J. Als-Nielsen, L. Leiserowitz and M. Lahav, *J. Phys. Chem. B*, 1998, **102**, 761.

4 N. H. Mendelson, *Science*, 1992, **258**, 1633; S. A. Davis, S. L. Burkett, N. H. Mendelson and S. Mann, *Nature* (*London*), 1997, **385**, 420; W. Shenton, D. Pum, U. B. Sleytr and S. Mann, *Nature* (*London*), 1997, **389**, 585; M. Field, C. J. Smith, D. D. Awschalom, N. H. Mendelson, E. L. Mayes, S. A. Davis and S. Mann, *Appl. Phys. Lett.*, 1998, **73**, 1739.

5 C. T. Kresge, M. E. Leonowicz, W. J. Roth, J. C. Vartuli and J. S. Beck, *Nature* (*London*), 1992, **359**, 710; D. Walsh, J. D. Hopwood and S. Mann, *Science*, 1994, **264**, 1576; D. Walsh and S. Mann, *Nature* (*London*), 1995, **377**, 320; Q. Hue, R. Leon, P. M. Petroff and G. D. Stucky, *Science*, 1995, **268**, 1324.

6 J. Lin, E. Cates and P. A. Bianconi, *J. Am. Chem. Soc.*, 1994, **116**, 4738; T. L. Morkved, P. Wiltzius, H. M. Jaeger, D. G. Grier and T. A. Witten, *Appl. Phys. Lett.*, 1994, **64**, 422; L. H. Radzilowski, B. O. Carragher and S. I. Stupp, *Macromolecules*, 1997, **30**, 2110; S. I. Stupp, *Curr. Opinion Colloid Interface Sci.*, 1998, **3**, 20; M. Templin, A. Franck, A. DuChesne, H. Leist, Y. M. Zhang, R. Ulrich, V. Schadler and U. Wiesner, *Science*, 1997, **278**, 1795.

7 A. Kumar and G. M. Whitesides, *Appl. Phys. Lett.*, 1993, **63**, 2002; A. Kumar, H. A. Biebuyck and G. M. Whitesides, *Langmuir*, 1994, **10**, 1498; A. Kumar, N. L. Abbott, E. Kim, H. A. Biebuyck and G. M. Whitesides, *Acc. Chem. Res.*, 1995, **28**, 219; J. L. Wilbur, A. Kumar, H. A. Biebuyck, E. Kim and G. M. Whitesides, *Nanotechnology*, 1996, **7**, 452; Y. N. Xia and G. M. Whitesides, *Annu. Rev. Mater. Sci.*, 1998, **28**, 153; X. M. Zhao, Y. N. Xia and G. M. Whitesides, *J. Mater. Chem.*, 1997, **7**, 1069.

8 A. Bernard, E. Delamarche, H. Schmid, B. Michel, H. R. Bosshard and H. Biebuyck, *Langmuir*, 1998, **14**, 2225; A. T. A. Jenkins, N. Boden, R. J. Bushby, S. D. Evans, P. F. Knowles, R. E. Miles, S. D. Ogier, H. Schonherr and G. J. Vancso, *J. Am. Chem. Soc.*, 1999, **121**, 5274; M. Mrksich and G. M. Whitesides, *Trends Biotechnol.*, 1995, **13**, 228; M. Mrksich, C. S. Chen, Y. N. Xia, L. E. Dike, D. E. Ingber and G. M. Whitesides, *Proc. Natl. Acad. Sci. USA*, 1996, **93**, 10775; S. G. Zhang, L. Yan, M. Altman, M. Lassle, H. Nugent, F. Frankel, D. A. Lauffenburger, G. M. Whitesides and A. Rich, *Biomaterials*, 1999, **20**, 1213.

9 A. Kumar and G. M. Whitesides, *Science*, 1994, **263**, 60.

10 S. L. Clark, M. Montague and P. T. Hammond, *Supramol. Sci.*, 1997, **4**, 141; Z. Y. Huang, P. C. Wang, A. G. MacDiarmid, Y. N. Xia and G. Whitesides, *Langmuir*, 1997, **13**, 6480.

11 P. G. Clem, N. L. Jeon, R. G. Nuzzo and D. A. Payne, *J. Am. Chem. Soc.*, 1997, **80**, 2821; P. C. Hidber, W. Helbig, E. Kim and G. M. Whitesides, *Langmuir*, 1996, **12**, 1375; N. L. Jeon, P. G. Clem, R. G. Nuzzo and D. A. Payne, *J. Mater. Res.*, 1995, **10**, 2996; N. L. Jeon, R. G. Nuzzo, Y. N. Xia, M. Mrksich and G. M. Whitesides, *Langmuir*, 1995, **11**, 3024; N. L. Jeon, P. G. Clem, D. A. Payne and R. G. Nuzzo, *Langmuir*, 1996, **12**, 5350; N. L. Jeon, W. B. Lin, M. K. Erhardt, G. S. Girolami and R. G. Nuzzo, *Langmuir*, 1997, **13**, 3833; S. Palacin, P. C. Hidber, J. P. Bourgoin, C. Miramond, C. Fermon and G. M. Whitesides, *Chem. Mater.*, 1996, **8**, 1316; T. Pompe, A. Fery, S. Herminghaus, A. Kriele, H. Lorenz and J. P. Kotthaus, *Langmuir*, 1999, **15**, 2398.

12 J. Aizenberg, A. J. Black and G. M. Whitesides, *Nature* (*London*), 1999, **398**, 495.

13 J. Aizenberg, A. J. Black and G. H. Whitesides, *J. Am. Chem. Soc.*, 1999, **121**, 4500.

14 Y. N. Xia and G. M. Whitesides, *Adv. Mater.*, 1995, **7**, 471; H. A. Biebuyck, N. B. Larsen, E. Delamarche and B. Michel, *IBM J. Res. Dev.*, 1997, **41**, 159; I. Bohm, A. Lampert, M. Buck, F. Eisert and M. Grunze, *Appl. Surf. Sci.*, 1999, **141**, 237; E. Delamarche, H. Schmid, A. Bietsch, N. B. Larsen, H. Rothuizen, B. Michel and H. Biebuyck, *J. Phys. Chem. B*, 1998, **102**, 3324; N. L. Jeon, K. Finnie, K. Branshaw and R. G. Nuzzo, *Langmuir*, 1997, **13**, 3382; N. B. Larsen, H. Biebuyck, E. Delamarche and B. Michel, *J. Am. Chem. Soc.*, 1997, **119**, 3017.
15 J. Aizenberg, A. J. Black and G. M. Whitesides, *Nature* (*London*), 1998, **394**, 868.
16 A. J. Black, K. E. Paul, J. Aizenberg and G. M. Whitesides, *J. Am. Chem. Soc.*, 1999, **121**, 8356.
17 A. Ulman, *An Introduction to Ultrathin Organic Films: From Langmuir–Blodgett to Self-Assembly*, Academic Press, Boston, 1991; R. G. Nuzzo, L. H. Dubois and D. L. Allara, *J. Am. Chem. Soc.*, 1990, **112**, 558; P. E. Laibinis, G. M. Whitesides, D. L. Allara, Y. T. Tao, A. N. Parikh and R. G. Nuzzo, *J. Am. Chem. Soc.*, 1991, **113**, 7152.
18 E. M. Landau, M. Levanon, L. Leiserowitz, M. Lahav and J. Sagiv, *Nature* (*London*), 1985, **318**, 353; E. M. Landau, S. G. Wolf, M. Levanon, L. Leiserowitz, M. Lahav and J. Sagiv, *J. Am. Chem. Soc.*, 1989, **111**, 1436; L. Addadi and S. Weiner, *Proc. Natl. Acad. Sci. USA*, 1985, **82**, 4110; L. Addadi, J. Moradian, E. Shay, N. G. Maroudas and S. Weiner, *Proc. Natl. Acad. Sci. USA*, 1987, **84**, 2732; S. Weiner and L. Addadi, *J. Mater. Chem.*, 1997, **7**, 689.
19 J. Aizenberg, Manuscript in preparation.
20 A.-L. Barabasi and H. E. Stanley, *Fractal Concepts in Surface Growth*, Cambridge University Press, Cambridge, 1995; K. Bromann, C. Felix, H. Brune, W. Harbich, R. Monot, J. Buttet and K. Kern, *Science*, 1996, **274**, 956; H. Brune, C. Romainczyk, H. Roder and K. Kern, *Nature* (*London*), 1994, **369**, 469.